JOC The Journal of Organic Chemistry

Article

pubs.acs.org/joc

Design of Fullerene Derivatives for Stabilizing LUMO Energy using Donor Groups Placed in Spatial Proximity to the C_{60} Cage

Fukashi Matsumoto,* Toshiyuki Iwai, Kazuyuki Moriwaki, Yuko Takao, Takatoshi Ito, Takumi Mizuno, and Toshinobu Ohno*

Osaka Municipal Technical Research Institute, 1-6-50 Morinomiya, Joto-ku, Osaka 536-8553, Japan

Supporting Information

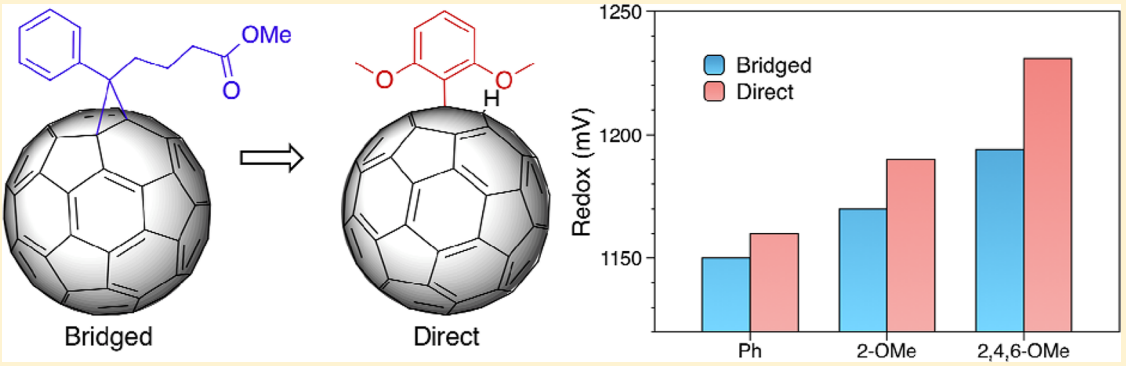

ABSTRACT: A series of arylated dihydrofullerene derivatives were synthesized to elucidate the effective design of fullerene derivatives for enhancing the performance of organic photovoltaics. The LUMO energy of the fullerenes was estimated by the first reduction potential and theoretical calculations. The results showed that the methoxy groups substituted at spatial proximity to the fullerene core offered significant stabilization of the LUMO level. The stabilizing effect of the directly arylated fullerenes is more significant than that of conventional methanofullerenes. The theoretical investigation was performed with regard to the electronic interaction between the methoxy and fullerene moieties.

INTRODUCTION

Due to the many potential applications of fullerenes in materials and nanotechnology, numerous fullerene derivatives have been synthesized in the past decade.[1] The excellent electron-accepting capability of fullerenes has made them promising materials for organic photovoltaics (OPVs).[2] OPVs have drawn considerable attention in recent years, owing to their advantages of low cost of fabrication, low weight, and suitability in developing flexible devices. The most prominently reported material system for bulk-heterojunction OPVs is the mixture of poly(3-hexylthiophene) and [6,6]-phenyl-C-61-butyric acid methyl ester (P3HT:PCBM).[3] Recently, there has been remarkable improvement in the device performance (up to 7−8%) of OPVs, due to the progress and development of new conjugated polymer donor materials.[4−7] However, research on novel C_{60}-based acceptor materials to replace PCBM has not been successful until now.[8−11] Investigation into the development of new acceptor materials is essential in order to realize significant improvement in device properties. Nevertheless, an efficient strategy for designing the acceptor materials has not yet been established.

It is empirically known that the open circuit voltage (V_{OC}) of OPVs is dictated by the relation[12]

$$V_{OC} = 1/e(|E^{D}(\mathrm{HOMO})| - |E^{A}(\mathrm{LUMO})|) - 0.3 \qquad (1)$$

where e is the elementary charge, $E^{D}(\mathrm{HOMO})$ is the highest occupied molecular orbital energy of the donor, and $E^{A}(\mathrm{LUMO})$ is the lowest unoccupied level of the acceptor. Therefore, the LUMO energy of the acceptor should lie at a shallow level to increase the V_{OC} value, unless the difference between the LUMOs of the donor and acceptor becomes lower than the exciton binding energy.[13] The higher level of the LUMO energy is easily achieved by increasing the number of substituents on a fullerene cage.[14] Blom et al. reported an increase in V_{OC} when [60]PCBM was replaced with its bis-adduct analogue.[15] Indene-C_{60} bis-adduct (ICBA) reported by Li et al., which possesses two indene substituents on a fullerene cage, also exhibited a higher LUMO energy level than PCBM. The V_{OC} and power-conversion efficiency of the P3HT-based OPVs reached 0.84 V and 5.44%, respectively.[16] However, the tris-adduct analogue of PCBM showed significantly reduced power-conversion efficiency due to the deterioration of electron transport in the fullerene phase.[17] These multiadducts fundamentally consist of various regioisomers. Therefore, the purification and isolation of these components is practically impossible and sometimes results in poor reproducibility of the device performance. This structural impurity introduces

Received: July 25, 2012
Published: October 4, 2012

   dx.doi.org/10.1021/jo3015159 | J. Org. Chem. 2012, 77, 9038−9043

disorder into the electronic energy levels, which could unfavorably affect the electronic properties of the device.[18]

In contrast, controlling the electronic properties of fullerene has been studied for a decade, focusing on modification of the substituents on the fullerene cage. Wudl et al. investigated through-space orbital interactions between the substituent and fullerene cage.[19] Hummelen et al. showed a significant change in the LUMO level, by substituting the phenyl ring of PCBM with electron-donating and electron-withdrawing substituents.[20] Although they aimed to verify the direct through-space effect of the phenyl substituent toward the fullerene core, they could not obtain experimental proof of it. They therefore concluded that the number of methoxy substituents, rather than the position of the substituents, is of importance. This result implied that the distance between the substituent and the fullerene cage was too large to realize a significant through-space effect, and there was still the possibility of increasing the V_{OC} by using the electron-donating group substituted at the closest proximity to the fullerene cage.

By employing the above assumption, we aimed to verify the largest direct through-space effect of a methoxy group on the fullerene cage, by designing a structure where the *o*-alkoxy phenyl group is directly substituted on the carbon cage, instead of the conventional methano-bridged substitution. To double the effect of the donating group, the 2,6-dialkoxyphenyl (DAP) moiety was selected as a key structure of the substituent (Figure 1). Preliminary DFT calculations reveal that this structure is

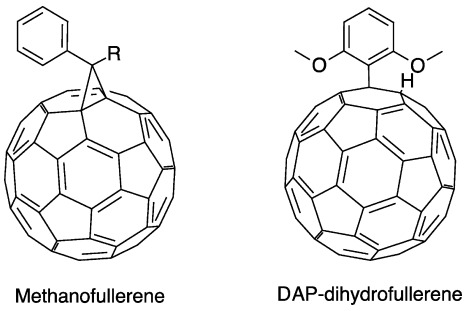

Figure 1. Schematic structures of the conventional and the newly designed fullerene derivatives.

effective in raising the LUMO energy and is therefore promising as a candidate for an acceptor material (vide infra). In this study, we synthesized a series of directly substituted fullerene derivatives and evaluated the effect of methoxy groups toward their energy level. Furthermore, their through-space effect was investigated by utilizing the natural localized molecular orbital (NLMO) analysis.

RESULTS AND DISCUSSION

Arylation of fullerenes, such as the Friedel–Crafts-type hydroarylation reaction, has been well studied by several groups.[21,22] For example, 1-(4-tolyl)-2-hydrofullerene can be obtained by the reaction of toluene and fullerene using $AlCl_3$ as a catalyst.[23] However, the target structure as described above could not be synthesized from *m*-dimethoxybenzene, which selectively afforded the 1-(2,4-dimethoxyphenyl)-2-hydrofullerene via electrophilic substitution. To synthesize the arylated fullerenes that possess methoxy groups at various positions of the phenyl group, we applied the procedure recently developed by Itami et al.[24] According to this report, arylated fullerenes were prepared by the rhodium-catalyzed coupling reaction of diverse arylboronic acids with fullerene (Table 1). The position of the substitution was completely directed by the boronic acid

Table 1. Synthesis of Arylated Fullerenes by Using Boronic Acids[a]

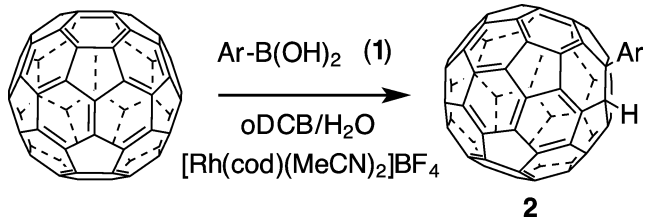

entry	Ar-B(OH)$_2$ (**1**)		yield of **2** (%)[b]
1	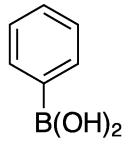	**1a**	49 (18)
2	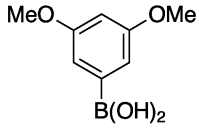	**1b**	47 (19)
3	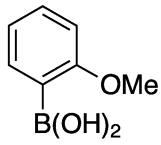	**1c**	63 (35)
4	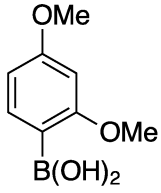	**1d**	60 (31)
5	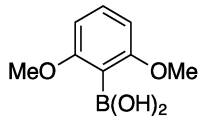	**1e**	75 (54)
6	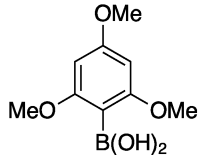	**1f**	78 (32)

[a]Conditions: 70 °C, 3 h, molar ratio C_{60}/**1**/Rh cat. = 1/1.2/0.1. [b]Yield determined from HPLC area ratio. Values in parentheses are isolated yields.

group. The reaction was performed at 70 °C for 3 h using 1.2 equiv of boronic acid with respect to C_{60}. Recycle preparative gel permeation chromatography (GPC) provided the purified products **2a–f**, and the structure of the obtained fullerenes was confirmed using ^{1}H and ^{13}C NMR, IR, and UV–vis spectroscopy and MALDI-TOF mass spectrometry. In the ^{1}H NMR spectra, the signal due to the hydrogen atom directly connected to the fullerene core appeared at approximately 6.7 ppm. The sharp absorption peak around 430 nm in the UV–vis spectrum of **2** is characteristic of 1,2-monoadducts of C_{60}.[25] The yields of the reaction were increased slightly from the

dx.doi.org/10.1021/jo3015159 | J. Org. Chem. 2012, 77, 9038–9043

nonsubstituted arylboronic acid (**2a**) to the trimethoxy-substituted acid (**2f**), because of the difference in the electron density on the aryl moiety. Unfortunately, the isolated yields were low (20−50%) due to the difficulty in purification, which arose from low solubility (<1 mg mL^{-1} in chloroform) of the products.

As a preliminary investigation on the effect of the methoxy group, the LUMO energies of the substituted fullerenes were predicted using DFT calculations and estimated by electrochemical measurements. Geometry-optimized structures of the products **2a**−**f** were performed using a DFT calculation program with the PBE functional and the DNP basis set as isolated molecules in vacuo. The LUMO energies obtained with this calculation level are shown in Figure 2 (right-hand axis).

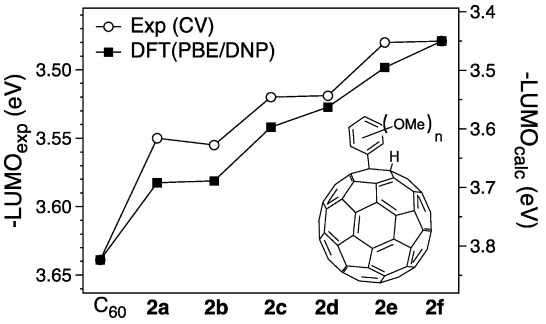

Figure 2. LUMO energies of C_{60} and arylated fullerenes (**2a**−**f**), estimated from the first reduction potentials measured by cyclic voltammetry (left axis, open circles), and theoretical values by DFT calculation at the PBE/DNP level (right axis, filled squares).

The electrochemical properties of the directly arylated fullerenes **2** were studied by cyclic voltammetry (CV) at room temperature in *o*-dichlorobenzene (oDCB). The experiments were carried out using 0.1 M tetra-*n*-butylammonium perchlorate as the supporting electrolyte with a Ag/Ag^+ reference electrode, platinum working electrode, platinum-wire counter electrode, and ferrocene/ferrocenium internal reference. All compounds showed three or four reversible electroreductions in the potential range from 0 to −2.0 V. It is assumed that the redox potential of the Fc/Fc^+ couple has an absolute energy level of −4.80 eV relative to vacuum. The LUMO energy was calculated according to the equation

$$E_{LUMO} = -(4.80 + \phi_{red}) \quad (eV) \qquad (2)$$

where ϕ_{red} is the first half-wave reduction potentials of the fullerenes **2a**−**f** relative to Fc/Fc^+.

As shown in Figure 2, similar trends were observed in the experimental and calculated LUMO energies, although the theoretical energies are overestimated in comparison to the experimental values. From these data, it can be concluded that the methoxy groups substituted in the ortho position are effective for raising the LUMO energy (**2c**,**e**). As expected from the calculations and general considerations, the para-substituted methoxy on the phenyl group provides a significant effect on the energy level. However, the experimental values of the para-substituted products (**2d**,**f**) did not change considerably from those for the unsubstituted products (**2c**,**e**). Further theoretical investigations were therefore performed to address this issue.

Musgrave et al. indicated that the results of the calculation with the time-dependent density functional theory (TD-DFT) for estimating LUMO energy were more accurate than the results of the direct estimation of the LUMO energy from the first unoccupied Kohn−Sham orbital.[26] According to this report, the LUMO energy was derived by adding the energy of the first singlet excitation calculated using TD-DFT to the HOMO energy of the highest occupied Kohn−Sham orbital at the DFT level calculation.

Previous work showed good correlation between the LUMO energies obtained by calculation for isolated molecules in vacuo and the redox potentials,[27] despite the fact that the CV measurements were performed in solution. However, the solvation effect cannot be neglected because the dipole moment from the solvent creates an induced dipole on the molecules, which may influence electron affinity of the fullerenes. Therefore, the conductor-like screening model (COSMO) was used to simulate the solvation environment of the fullerenes during CV measurements, applying the dielectric constant of oDCB (ε = 10.12).[28]

As shown in Figure 3, a strong linear correlation of the calculated LUMO energies with the experimental values was

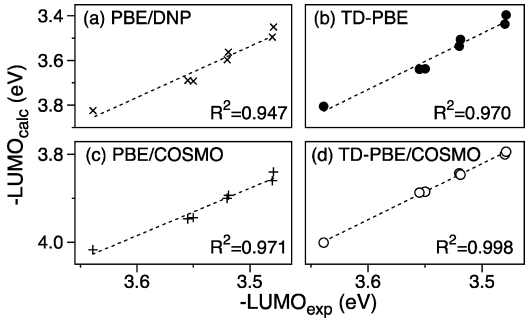

Figure 3. Plots of the experimental LUMO energy levels versus theoretical values. The LUMO levels are calculated by (a) PBE/DNP, (b) PBE/DNP with TD-DFT, (c) PBE/DNP with COSMO, and (d) PBE/DNP with TD-DFT/COSMO methods. R^2 = squared correlation coefficient for the fit.

verified. The squared correlation coefficients reported inside the plots indicate that the calculation from the combined TD-DFT (Figure 3b) and COSMO methods (Figure 3c) gave better results than a simple DFT calculation (Figure 3a). Furthermore, applying time-dependent DFT calculations with the inclusion of solvation effects provides a strong correlation (Figure 3d). These results indicate that the DFT calculation utilizing the simultaneous TD-DFT/COSMO method is appropriate for reproducing the results of CV measurements in solvent environments. The disagreement in the experimental and theoretical LUMO values for the para-substitution of the phenyl group in Figure 2 could be attributed to the solvation effect of oDCB. The estimation of LUMO energy using the reduction potential can be performed; however, this should be done with a solid-state measurement, such as inverse photoelectron spectroscopy (IPES),[29] for precise determination. Nevertheless, we concluded that the methoxy groups substituted in the ortho-position are more effective than the para-position and that the estimation of LUMO levels using DFT calculations is useful for designing novel acceptor materials.

Figure 4 shows the absorption spectra of the obtained fullerenes in chloroform at room temperature. A sharp absorption peak was observed around 430 nm, and this is minimally shifted toward longer wavelengths with an increasing number of methoxy substituents on the phenyl ring. This result

dx.doi.org/10.1021/jo3015159 | J. Org. Chem. 2012, 77, 9038−9043

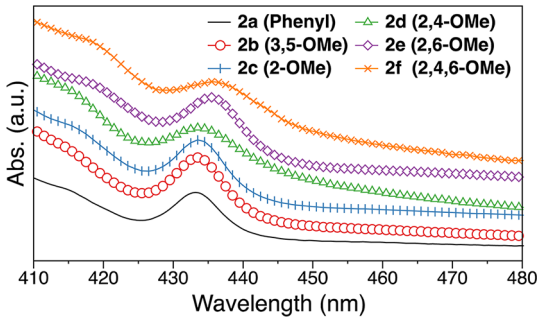

Figure 4. UV−vis absorption spectra of arylated fullerenes (**2a**−**f**) in chloroform.

indicates that elevated LUMO energy levels of the arylated fullerenes are accomplished without decreasing the band gap.

Figure 5 displays the calculated surface plots of the HOMO and LUMO energies for compound **2e**. A majority of the

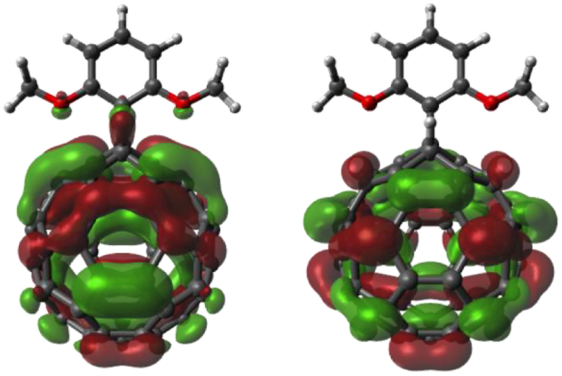

Figure 5. HOMO (left) and LUMO (right) surface plots for **2e** computed using B3LYP/6-31G(d).

HOMO and LUMO is located on the fullerene cage with a small amount on the oxygen atom. This suggests there are weak interactions between the methoxy group and the cage; however, there is minimal electron transfer from the 2,6-dimethoxyphenyl group to the fullerene moiety. Therefore, it can be proposed that the DAP structure plays a key role in adjusting the level of the LUMO without creating the charge transfer (CT) trap bands, which would interfere with efficient photoelectric conversion.

To further verify the effect of the methoxy groups substituted at the closest proximity to the fullerene cage, we compared a series of the first reduction potentials of the substituted methanofullerenes (bridged type) with the arylated fullerenes (direct type) (Figure 6). The literature values for the methanofullerenes[20] and the observed values of the arylated fullerenes were normalized by utilizing PCBM as the standard. Understandably, the stabilization of LUMO energy in arylated fullerenes is substantially higher than that of methanofullerenes. It should also be noted that the value for the 2,4,6-methoxy-arylated fullerene **2f** is close to that of the PCBM bis-adduct.[15] The reasons for this phenomenon remain unclear; however, they should be discussed by taking into account the through-bond/through-space electronic effects. Because of the lack of direct conjugation between the phenyl group and the C_{60} core, the through-bond effect appears to be relatively weak; therefore, we focused on studying the through-space effect between them.

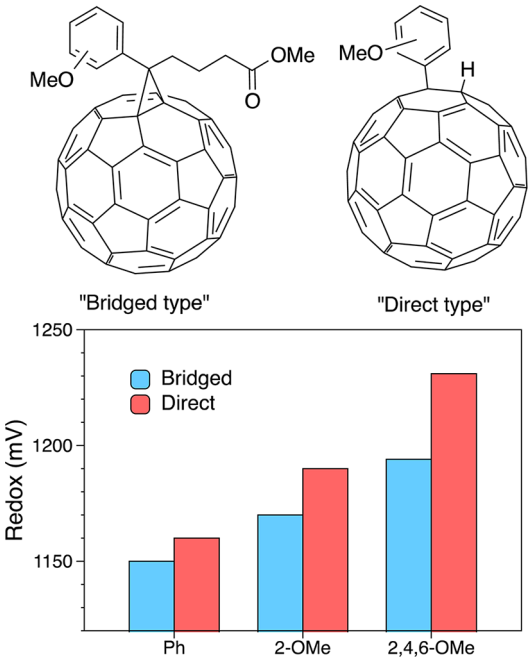

Figure 6. Comparison of first reduction potentials of methanofullerenes (bridged type) and arylated fullerenes (direct type). The values of bridged-type fullerenes were obtained by Hummelen et al.[20]

Considering the theoretically optimized structure of the arylated fullerene **2e**, the oxygen lone pair points toward the surface of the fullerene π system; this facilitates good electronic overlap between them. To analyze the mechanism of the LUMO stabilization, natural localized molecular orbital (NLMO) analysis[30] was employed for the optimized structures at the B3LYP/6-31G(d) level. Figure 7 depicts the NLMO of

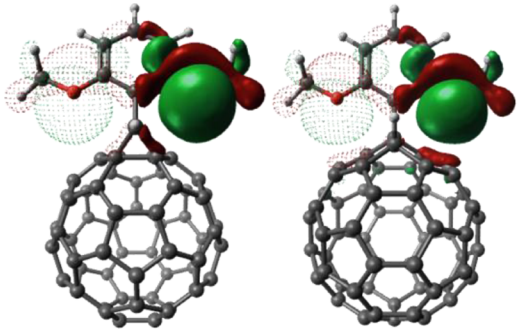

Figure 7. Three-dimensional images of the natural localized molecular orbital (NLMO) for the delocalization of the oxygen lone pair for the bridged-type (left) and the direct-type (right) models.

the lone pair on oxygen for the model structures of the bridged- and direct-type fullerenes. Table 2 summarizes the contribution of the atomic orbitals, which belong to the C_{60} cage, oxygen, and other moieties such as phenyl and methyl groups, to the

Table 2. Contributions of Atomic Orbitals of Each Moiety for the NLMO in Figure 7

model	C_{60} core (%)	oxygen (%)	others (%)[a]
bridged type	0.07	98.37	1.56
direct type	0.23	98.20	1.57

[a]Orbitals on phenyl and methyl groups.

dx.doi.org/10.1021/jo3015159 | J. Org. Chem. 2012, 77, 9038−9043

NLMO. The majority of the electron density from the lone pair electrons is strongly localized on the oxygen. Nevertheless, the contribution of the fullerene core is more significant in the direct-type than in the bridged-type model. This indicates a stronger interaction between the lone pair and the π electrons on the fullerene cage. From this prediction, we concluded that the LUMO energy of the directly arylated fullerenes was stabilized to some extent by the through-space effect between the methoxy group and the fullerene core.

CONCLUSION

We developed a new design for an effective acceptor material for OPVs characterized by the 2,6-dimethoxyphenyl group directly substituted on the fullerene cage. The methoxy groups placed at closest proximity to the fullerene core offer a distinct advantage over conventional methanofullerenes in the stabilization of LUMO energies, due to the through-space interaction between the methoxy and fullerene moieties. To further understand the though-space effect, the derivatives containing other substituents, such as amino groups, will be investigated in future work. The newly designed structure is therefore a promising alternative for enhancing the voltage of OPVs. The application of this new class of fullerene derivatives on OPVs is under way, and it will be reported in future publications. In addition, we observed an enhanced V_{OC} of 0.8 V using P3HT and a derivative of **2e** in primitive devices.

EXPERIMENTAL SECTION

General Methods. Reduction potentials were determined by cyclic voltammetry (CV) using a platinum working electrode, platinum-wire counter electrode, and Ag/Ag^+ reference electrode. Measurements were performed under Ar gas; an *o*-dichlorobenzene solution containing tetrabutylammonium perchlorate (0.1 M) was used as a supporting electrolyte, and the scan rate was 20 mV/s at room temperature. ^{1}H NMR and ^{13}C NMR spectra were recorded using a 300 MHz instrument in deuterated solvents with tetramethylsilane as an internal reference. Mass spectra were obtained using matrix-assisted laser desorption ionization time-of-flight mass spectrometry (MALDI TOF-MS). HPLC analyses were performed using toluene/methanol as an eluent. 2,4,6-Trimethoxyphenylboronic acid[31] and 1-phenyl-1,9-dihydro[60]fullerene (**2a**)[24] were prepared according to the literature. All the other solvents and materials are commercially available and were used as received.

General Procedure for Synthesis of Arylated Fullerenes. *1-(3,5-Dimethoxyphenyl)-1,9-dihydro[60]fullerene (**2b**).* The compound was prepared by a modified experimental procedure of the literature.[24] In a 50 mL flask were added 3,5-dimethoxyphenylboronic acid (30.3 mg, 0.167 mmol), $[Rh(cod)(MeCN)_2]BF_4$ (5.20 mg, 13.8 μmol), and C_{60} (100 mg, 0.139 mmol). Then *o*-dichlorobenzene (17.0 mL) and H_2O (4.20 mL) were added under a stream of argon. After the mixture was stirred at 70 °C for 3 h, it was extracted with toluene. The organic layer was dried over $NaSO_4$ and concentrated in vacuo. The residue was purified by recycle preparative gel permeation chromatography and centrifuged with methanol to afford **2b** (22 mg, 19% yield) as a dark brown powder. ^{1}H NMR (300 MHz, CS_2/$CDCl_3$): δ 7.52 (d, 2H, J = 1.8 Hz), 6.73 (s, 1H), 6.62 (t, 1H, J = 2.1 Hz), 4.00 (s, 6H). ^{13}C NMR (75 MHz, CS_2/$CDCl_3$): δ 162.04, 153.51, 152.39, 150.15, 147.45, 146.86, 146.29, 146.12, 145.89, 145.73, 145.46, 145.33, 144.57, 144.47, 143.19, 142.53, 142.23, 142.01, 141.87, 141.57, 141.51, 140.10, 135.77, 106.21, 99.32, 67.90, 63.68, 55.47. FT-IR (KBr): 2919, 1457, 1428, 1375, 1259, 1031, 754, 526 cm^{-1}. HRMS (MALDI-TOF, negative): m/z calcd for $C_{68}H_{10}O_2$ [M$^-$] 858.0681, found 858.0691.

*1-(2-Methoxyphenyl)-1,9-dihydro[60]fullerene (**2c**):* dark brown powder; 40 mg, 35% yield; ^{1}H NMR (300 MHz, CS_2/$CDCl_3$) δ 8.15 (dd, 1H, J = 7.5, 1.5 Hz), 7.57 (ddd, 1H, J = 7.8, 7.8, 1.8 Hz), 7.32 (d, 1H, J = 8.1 Hz), 7.22 (ddd, 1H, J = 7.5, 7.5, 1.2 Hz), 6.73 (s, 1H), 4.23 (s, 3H); ^{13}C NMR (75 MHz, CS_2/$CDCl_3$) δ 157.87, 153.70, 153.40, 147.19, 146.93, 146.78, 146.05, 145.99, 145.85, 145.82, 145.56, 145.27, 145.05, 144.57, 144.34, 143.00, 142.34, 142.29, 141.90, 141.82, 141.44, 141.35, 139.98, 139.70, 136.50, 135.67, 129.91, 128.54, 121.32, 111.84, 66.15, 61.89, 55.12; FT-IR (KBr) 2924, 2827, 1590, 1455, 1421, 1312, 1203, 1158, 1055, 526 cm^{-1}; HRMS (MALDI-TOF, negative) m/z calcd for $C_{67}H_8O$ [M$^-$] 828.0575, found 828.0580.

*1-(2,4-Dimethoxyphenyl)-1,9-dihydro[60]fullerene (**2d**):* dark brown powder; 37 mg, 31% yield; ^{1}H NMR (300 MHz, CS_2/$CDCl_3$) δ 8.04 (d, 1H, J = 8.4 Hz), 6.86 (d, 1H, J = 2.7 Hz), 6.71 (s, 1H), 6.70 (dd, 1H, J = 8.7, 2.7 Hz), 4.27 (s, 3H), 3.95 (s, 3H); ^{13}C NMR (75 MHz, CS_2/$CDCl_3$) δ 161.21, 158.91, 153.88, 147.27, 146.85, 146.10, 145.92, 145.65, 145.27, 145.16, 144.64, 144.13, 143.05, 142.39, 142.01, 141.88, 141.57, 141.40, 139.99, 139.79, 136.57, 136.44, 129.01, 128.63, 104.26, 100.13, 65.71, 62.02, 55.27, 55.08; FT-IR (KBr) 2926, 2828, 1605, 1500, 1458, 1207, 1031, 818, 526 cm^{-1}; HRMS (MALDI-TOF, negative) m/z calcd for $C_{68}H_{10}O_2$ [M$^-$] 858.0681, found 858.0685.

*1-(2,6-Dimethoxyphenyl)-1,9-dihydro[60]fullerene (**2e**):* dark brown powder; 64 mg, 54% yield; ^{1}H NMR (300 MHz, CS_2/$CDCl_3$) δ 7.46 (t, 1H, J = 8.4 Hz), 6.92 (d, 2H, J = 8.4 Hz), 6.69 (s, 1H), 4.06 (s, 6H); ^{13}C NMR (75 MHz, CS_2/$CDCl_3$) δ 158.73, 155.77, 154.68, 147.09, 146.09, 145.92, 145.85, 145.15, 144.91, 144.72, 144.57, 143.20, 142.39, 142.32, 142.06, 141.78, 141.48, 141.29, 139.10, 137.20, 134.81, 129.66, 128.82, 128.06, 106.48, 63.53, 63.22, 55.93; FT-IR (KBr) 2924, 1578, 1469, 1427, 1245, 1109, 515 cm^{-1}; HRMS (MALDI-TOF, negative) m/z calcd for $C_{68}H_{10}O_2$ [M$^-$] 858.0681, found 858.0689.

*1-(2,4,6-Trimethoxyphenyl)-1,9-dihydro[60]fullerene (**2f**):* dark brown powder; 40 mg, 32% yield; ^{1}H NMR (300 MHz, CS_2/$CDCl_3$) δ 6.67 (s, 1H), 6.43 (s, 2H), 4.04 (s, 6H), 3.95 (s, 3H); ^{13}C NMR data could not be obtained due to the extremely low solubility; FT-IR (KBr) 2928, 1603, 1459, 1340, 1205, 1128, 811 cm^{-1}; HRMS (MALDI-TOF, negative) m/z calcd for $C_{69}H_{12}O_3$ [M$^-$] 888.0786, found 888.0788.

Computational Details. Full geometry optimizations and TD-DFT calculations have been carried out at the PBE/DNP level in DMol^3 (Materials Studio, Accelrys).[32] The surface plots of HOMO and LUMO orbitals of **2e** were generated with the Gaussian 03 package[33] at the B3LYP/6-31G(d) level. NLMO analyses were performed for the model compounds at their optimized geometries at the B3LYP/6-31G(d) level, using the NBO 3.1 program.

ASSOCIATED CONTENT

Supporting Information

Figures and tables giving ^{1}H NMR, ^{13}C NMR, and MALDI-TOF HRMS spectra of new compounds **2b**–**2f**, cyclic voltammograms of fullerene derivatives, and computational details. This material is available free of charge via the Internet at http://pubs.acs.org.

AUTHOR INFORMATION

Corresponding Author

*E-mail: matumoto@omtri.or.jp (F.M.); ohno@omtri.or.jp (T.O.).

Notes

The authors declare no competing financial interest.

ACKNOWLEDGMENTS

This research was supported in part by Core Research for Evolutional Science and Technology (CREST) of the Japan Science and Technology Agency (JST) and JSPS KAKENHI Grant Number 23750232, 22550176.

REFERENCES

(1) Thilgen, C.; Diederich, F. *Chem. Rev.* **2006**, *106*, 5049–5135.

(2) Brabec, C. J.; Sariciftci, N. S.; Hummelen, J. C. *Adv. Funct. Mater.* **2001**, *11*, 15−26.
(3) Li, G.; Shrotriya, V.; Yao, Y.; Yang, Y. *J. Appl. Phys.* **2005**, *98*, 043704.
(4) Chen, H.-Y.; Hou, J.; Zhang, S.; Liang, Y.; Yang, G.; Yang, Y.; Yu, L.; Wu, Y.; Li, G. *Nat. Photonics* **2009**, *3*, 649−653.
(5) Su, M.-S.; Kuo, C.-Y.; Yuan, M.-C.; Jeng, U. S.; Su, C.-J.; Wei, K.-H. *Adv. Mater.* **2011**, *23*, 3315−3319.
(6) Price, S. C.; Stuart, A. C.; Yang, L.; Zhou, H.; You, W. *J. Am. Chem. Soc.* **2011**, *133*, 4625−4631.
(7) Piliego, C.; Holcombe, T. W.; Douglas, J. D.; Woo, C. H.; Beaujuge, P. M.; Fréchet, J. M. J. *J. Am. Chem. Soc.* **2010**, *132*, 7595−7597.
(8) Zhao, G.; He, Y.; Xu, Z.; Hou, J.; Zhang, M.; Min, J.; Chen, H.-Y.; Ye, M.; Hong, Z.; Yang, Y.; Li, Y. *Adv. Funct. Mater.* **2010**, *20*, 1480−1487.
(9) Kuhlmann, J.-C.; de Bruyn, P.; Bouwer, R. K. M.; Meetsma, A.; Blom, P. W. M.; Hummelen, J. C. *Chem. Commun.* **2010**, *46*, 7232−7234.
(10) Lee, H. S.; Yoon, S. C.; Lim, J.; Lee, M.; Lee, C. *J. Nanosci. Nanotechnol.* **2008**, *8*, 4533−4537.
(11) Lee, H. S.; Yoon, S. C.; Lim, J.; Lee, M.; Lee, C. *Mol. Cryst. Liq. Cryst.* **2008**, *492*, 657−666.
(12) Dennler, G.; Scharber, M. C.; Ameri, T.; Denk, P.; Forberich, K.; Waldauf, C.; Brabec, C. J. *Adv. Mater.* **2008**, *20*, 579−583.
(13) Thompson, B. C.; Kim, Y.-G.; McCarley, T. D.; Reynolds, J. R. *J. Am. Chem. Soc.* **2006**, *128*, 12714−12725.
(14) Niinomi, T.; Matsuo, Y.; Hashiguchi, M.; Sato, Y.; Nakamura, E. *J. Mater. Chem.* **2009**, *19*, 5804−5811.
(15) Lenes, M.; Wetzelaer, G.-J. A. H.; Kooistra, F. B.; Veenstra, S. C.; Hummelen, J. C.; Blom, P. W. M. *Adv. Mater.* **2008**, *20*, 2116−2119.
(16) He, Y.; Chen, H.-Y.; Hou, J.; Li, Y. *J. Am. Chem. Soc.* **2010**, *132*, 1377−1382.
(17) Lenes, M.; Shelton, S. W.; Sieval, A. B.; Kronholm, D. F.; Hummelen, J. C.; Blom, P. W. M. *Adv. Funct. Mater.* **2009**, *19*, 3002−3007.
(18) Frost, J. M.; Faist, M. A.; Nelson, J. *Adv. Mater.* **2010**, *22*, 4881−4884.
(19) Eiermann, M.; Haddon, R. C.; Knight, B.; Li, Q. C.; Maggini, M.; Martín, N.; Ohno, T.; Prato, M.; Suzuki, T.; Wudl, F. *Angew. Chem., Int. Ed. Engl.* **1995**, *34*, 1591−1594.
(20) Kooistra, F. B.; Knol, J.; Kastenberg, F.; Popescu, L. M.; Verhees, W. J. H.; Kroon, J. M.; Hummelen, J. C. *Org. Lett.* **2007**, *9*, 551−554.
(21) Chen, Z.-X.; Wang, G.-W. *J. Org. Chem.* **2005**, *70*, 2380−2383.
(22) Iwashita, A.; Matsuo, Y.; Nakamura, E. *Angew. Chem., Int. Ed. Engl.* **2007**, *46*, 3513−3516.
(23) Kokubo, K.; Tochika, S.; Kato, M.; Sol, Y.; Oshima, T. *Org. Lett.* **2008**, *10*, 3335−3338.
(24) Nambo, M.; Noyori, R.; Itami, K. *J. Am. Chem. Soc.* **2007**, *129*, 8080−8081.
(25) Meier, M.; Bergosh, R.; Gallagher, M.; Spielmann, H.; Wang, Z. *J. Org. Chem.* **2002**, *67*, 5946−5952.
(26) Zhang, G.; Musgrave, C. B. *J. Phys. Chem. A* **2007**, *111*, 1554−1561.
(27) Suzuki, T.; Maruyama, Y.; Akasaka, T.; Ando, W. *J. Am. Chem. Soc.* **1994**, *116*, 1359−1363.
(28) Tan, K.; Lu, X.; Wang, C.-R. *J. Phys. Chem. B* **2006**, *110*, 11098−11102.
(29) Akaike, K.; Kanai, K.; Ouchi, Y.; Seki, K. *Appl. Phys. Lett.* **2009**, *94*, 3309.
(30) Reed, A. E.; Weinhold, F. *J. Chem. Phys.* **1985**, *83*, 1736−1740.
(31) Chaumeil, H.; Signorella, S.; Le Drian, C. *Tetrahedron* **2000**, *56*, 9655−9662.
(32) Delley, B. *J. Chem. Phys.* **1991**, *94*, 7245−7251.
(33) Frisch, M. J., et al. *Gaussian 03, Revision C.02*; Gaussian, Inc., Wallingford, CT, 2004.